

## 1. NMR Spectrum of the prepared energetic salts

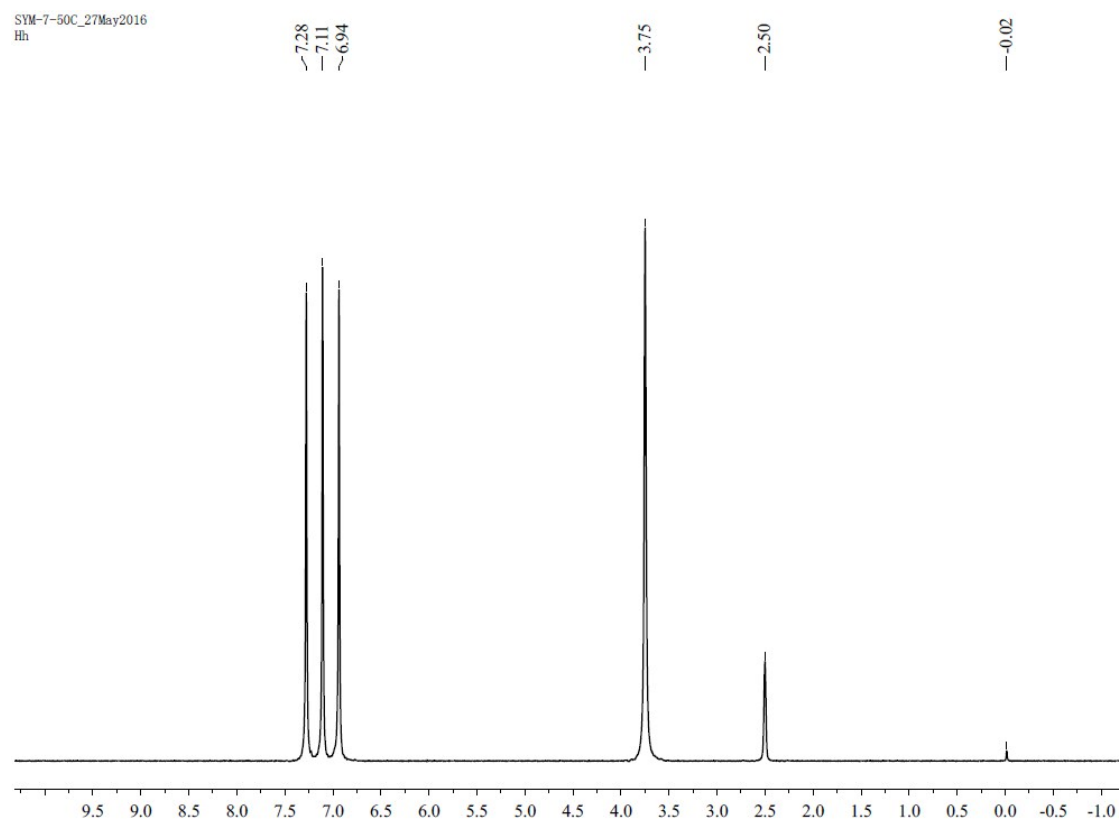


Figure S1. <sup>1</sup>H NMR spectrum of diammonium BNOA (6)

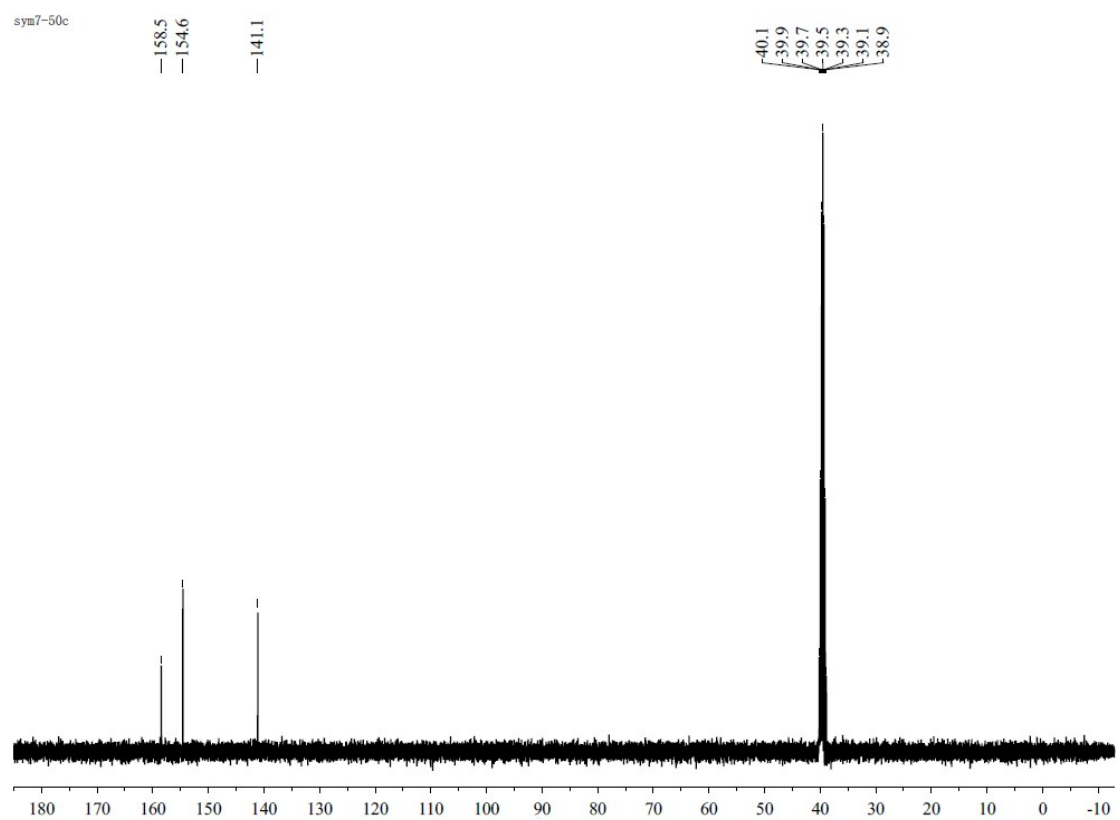


Figure S2.  $^{13}\text{C}$  NMR spectrum of diammonium BNOA (6)

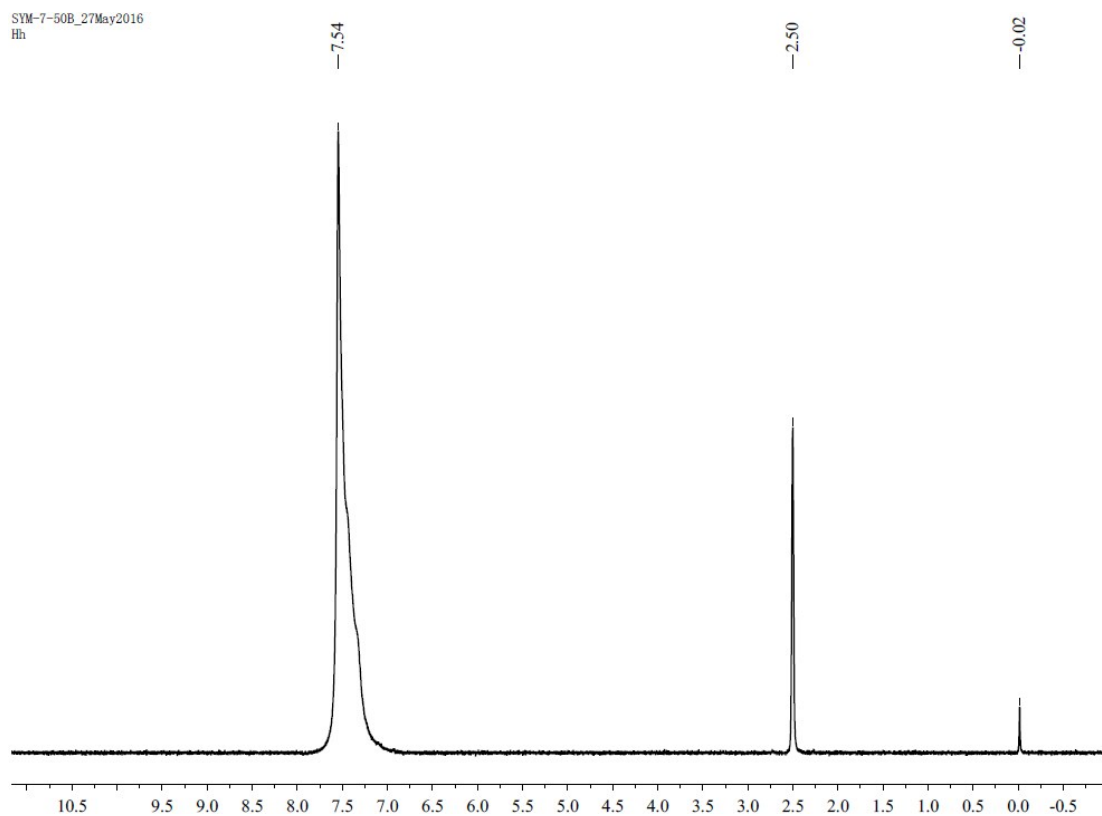


Figure S3.  $^1\text{H}$  NMR spectrum of dihydrazinium BNOA (7)

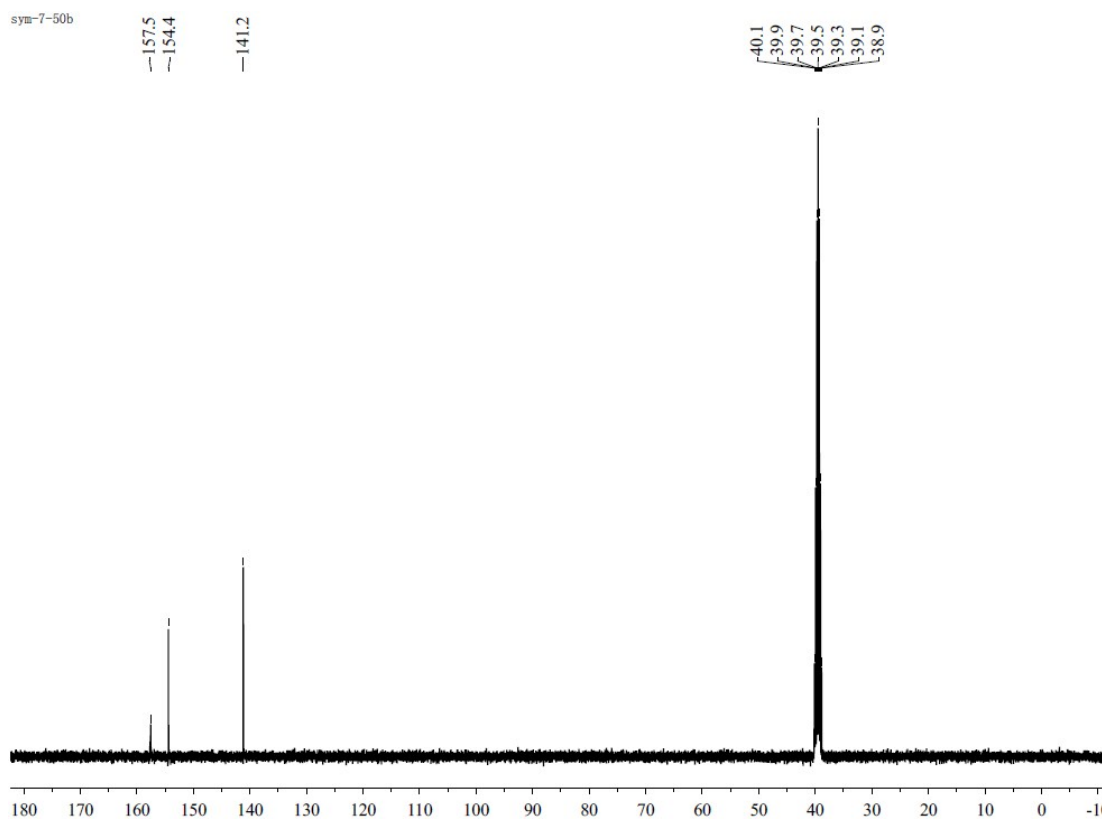


Figure S4.  $^{13}\text{C}$  NMR spectrum of dihydrazinium BNOA (7)

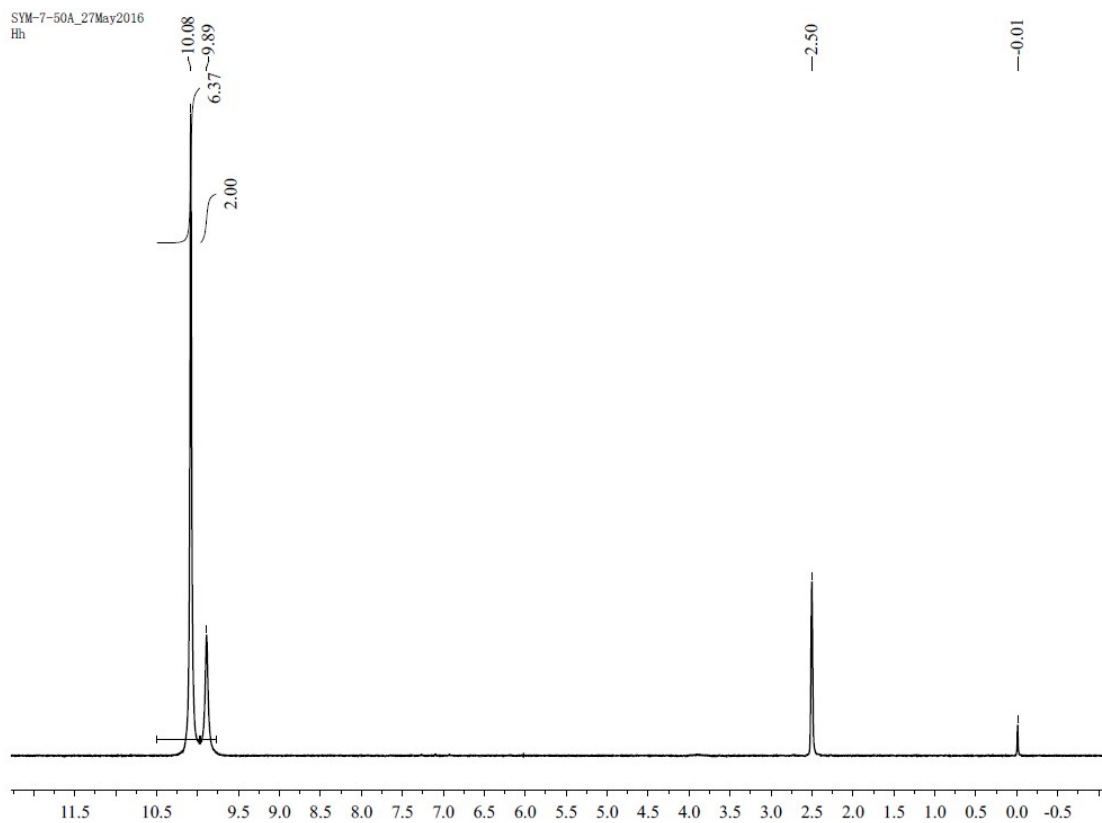


Figure S5.  $^1\text{H}$  NMR spectrum of dihydroxylammonium BNOA (**8**)

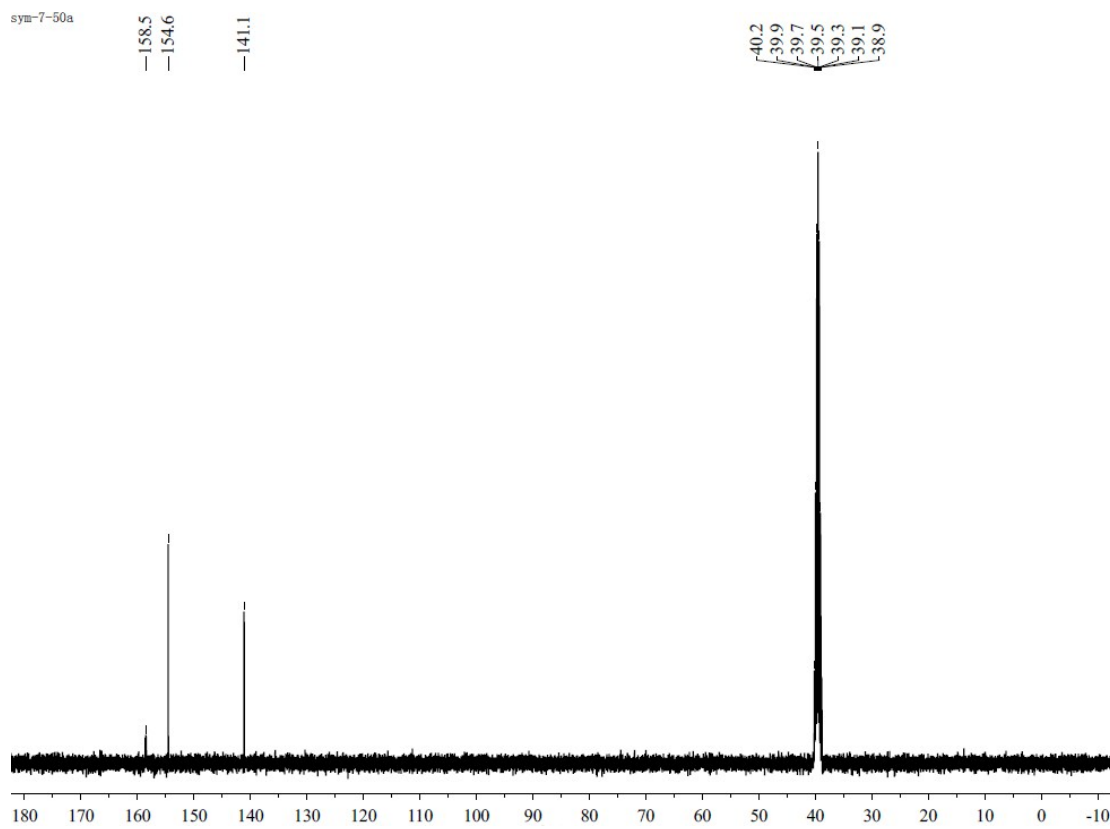


Figure S6.  $^{13}\text{C}$  NMR spectrum of dihydroxylammonium BNOA (**8**)

SYM-7-50D\_27May2016  
Hh

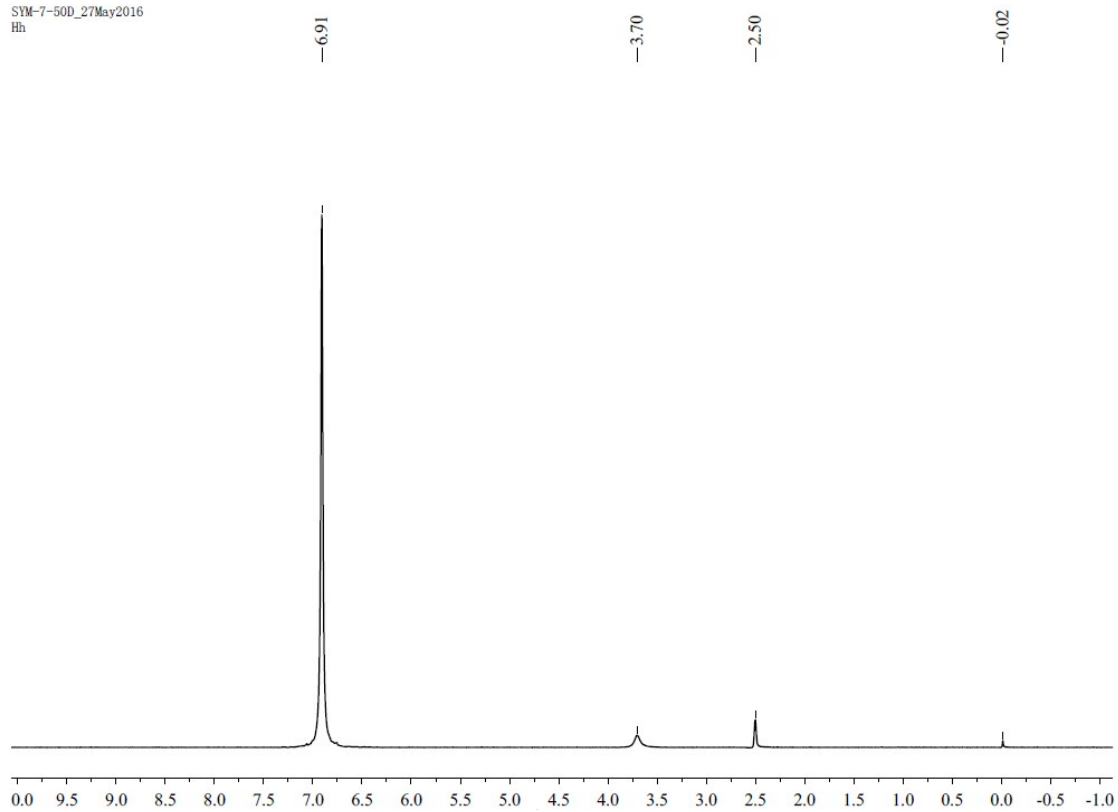


Figure S7. <sup>1</sup>H NMR spectrum of bis(guanidinium) BNOA (**9**)

sym7-50d

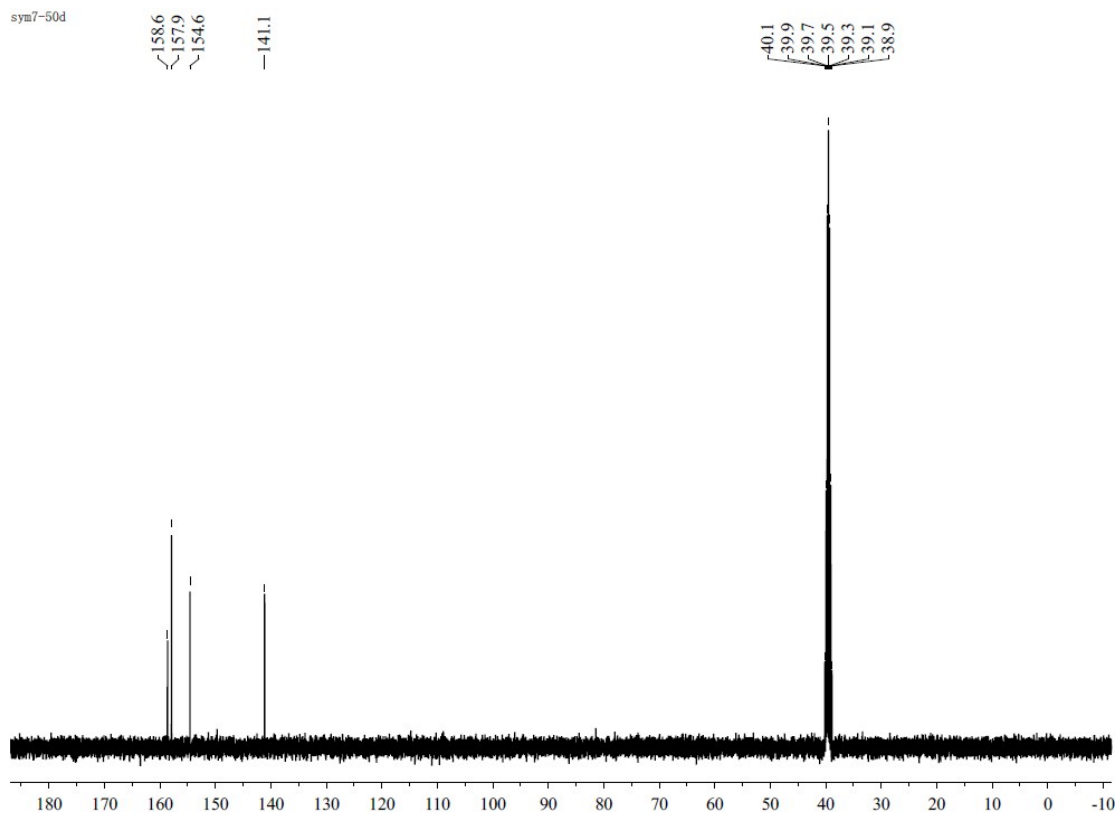


Figure S8. <sup>13</sup>C NMR spectrum of bis(guanidinium) BNOA (**9**)

SYM-7-51A\_27May2016  
Hh

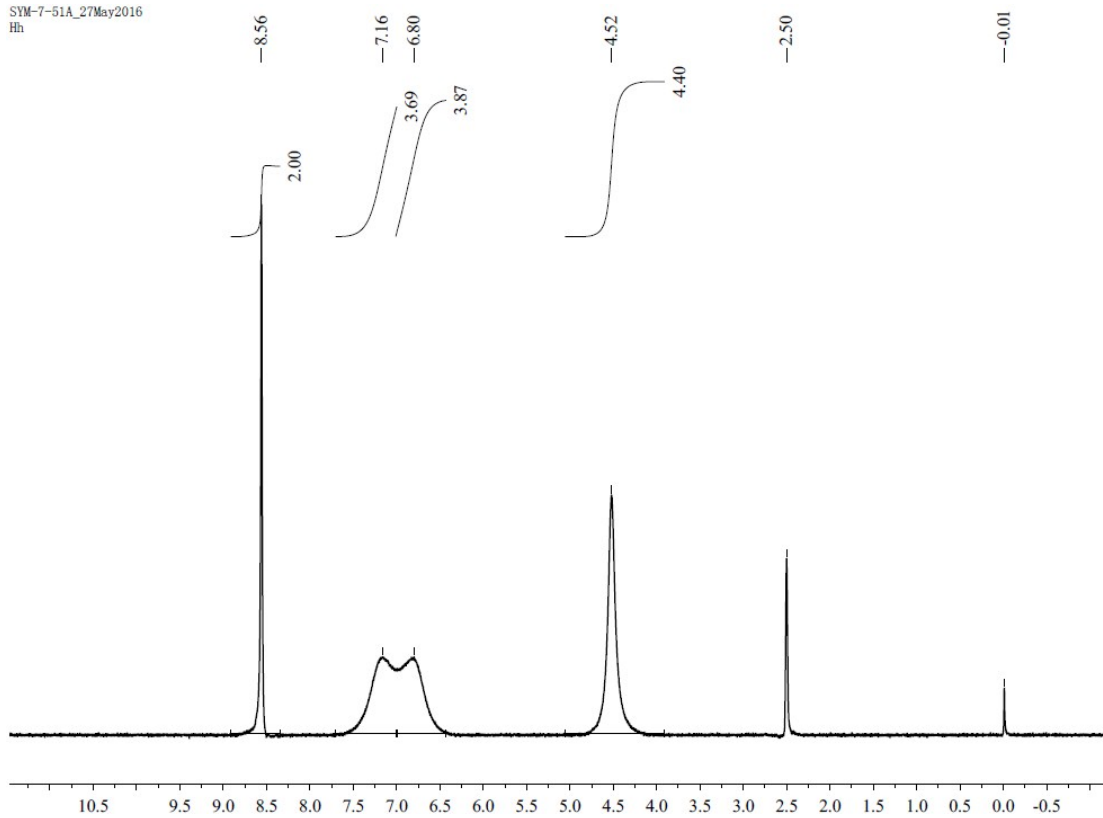


Figure S9. <sup>1</sup>H NMR spectrum of bis(aminoguanidinium) BNOA (**10**)

sym7-51a

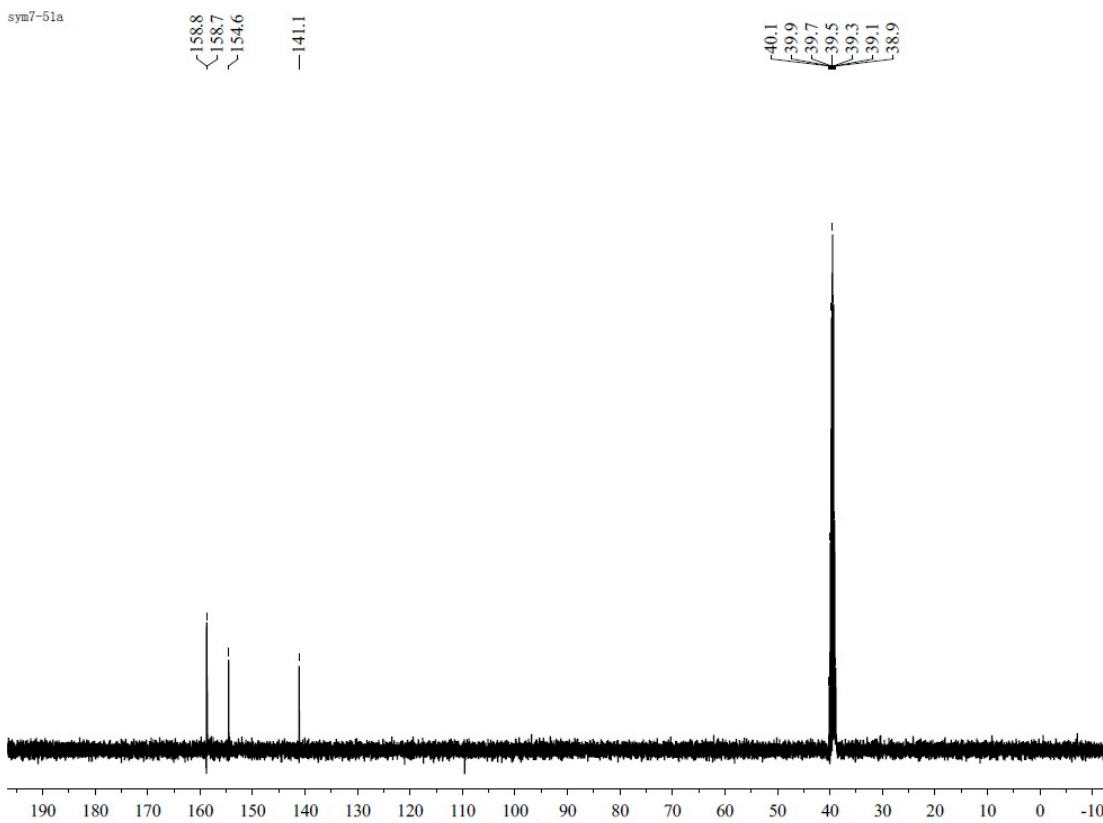


Figure S10. <sup>13</sup>C NMR spectrum of bis(aminoguanidinium) BNOA (**10**)

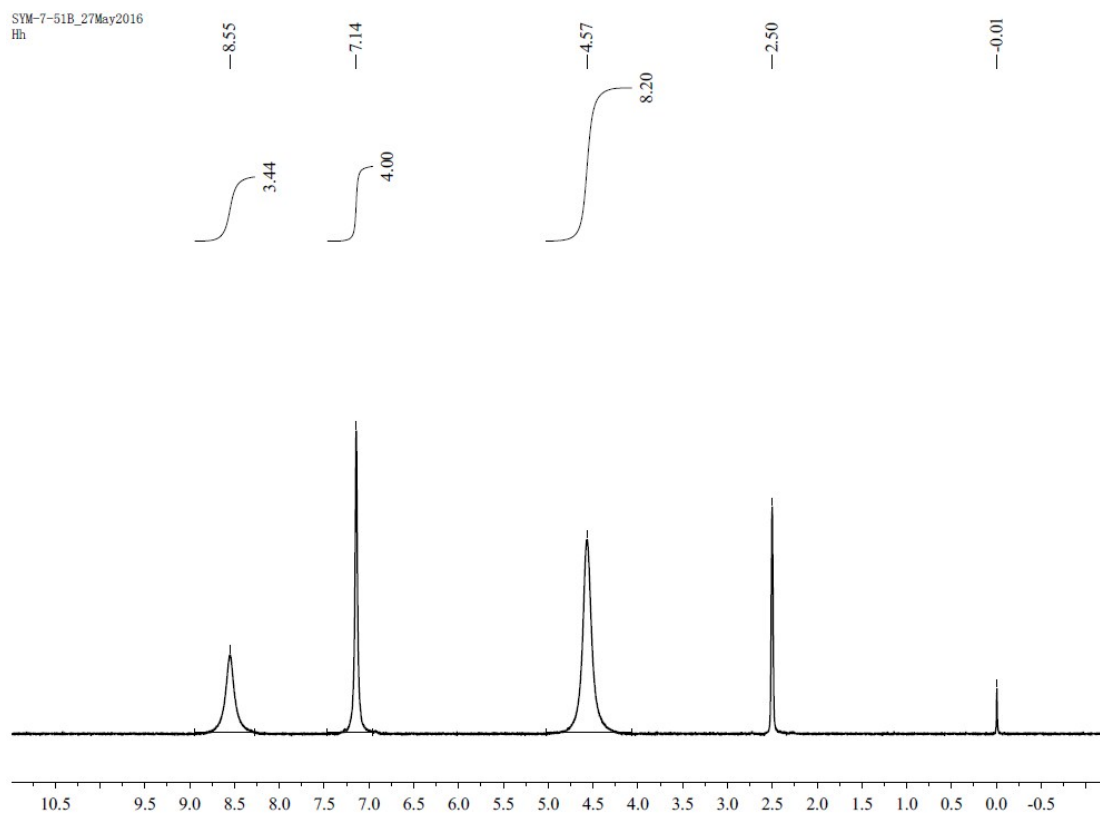


Figure S11.  $^1\text{H}$  NMR spectrum of bis(diaminoguanidinium) BNOA (**11**)

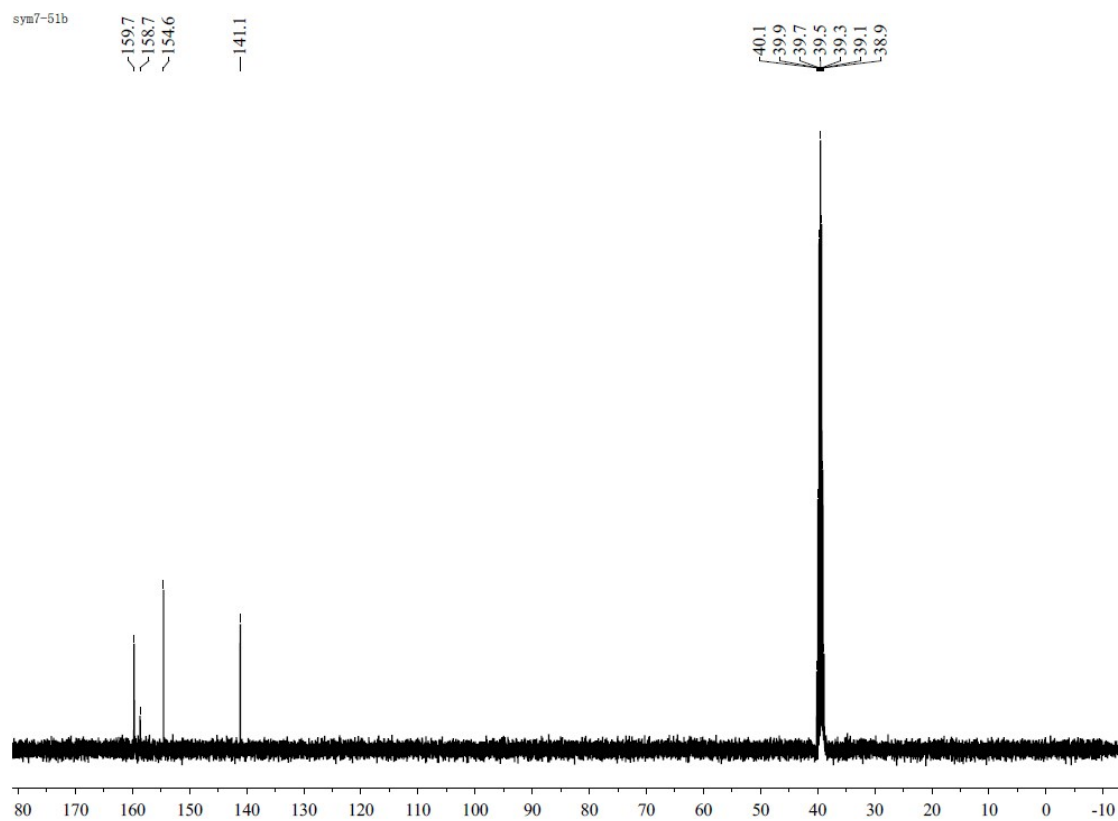


Figure S12.  $^{13}\text{C}$  NMR spectrum of bis(diaminoguanidinium) BNOA (**11**)

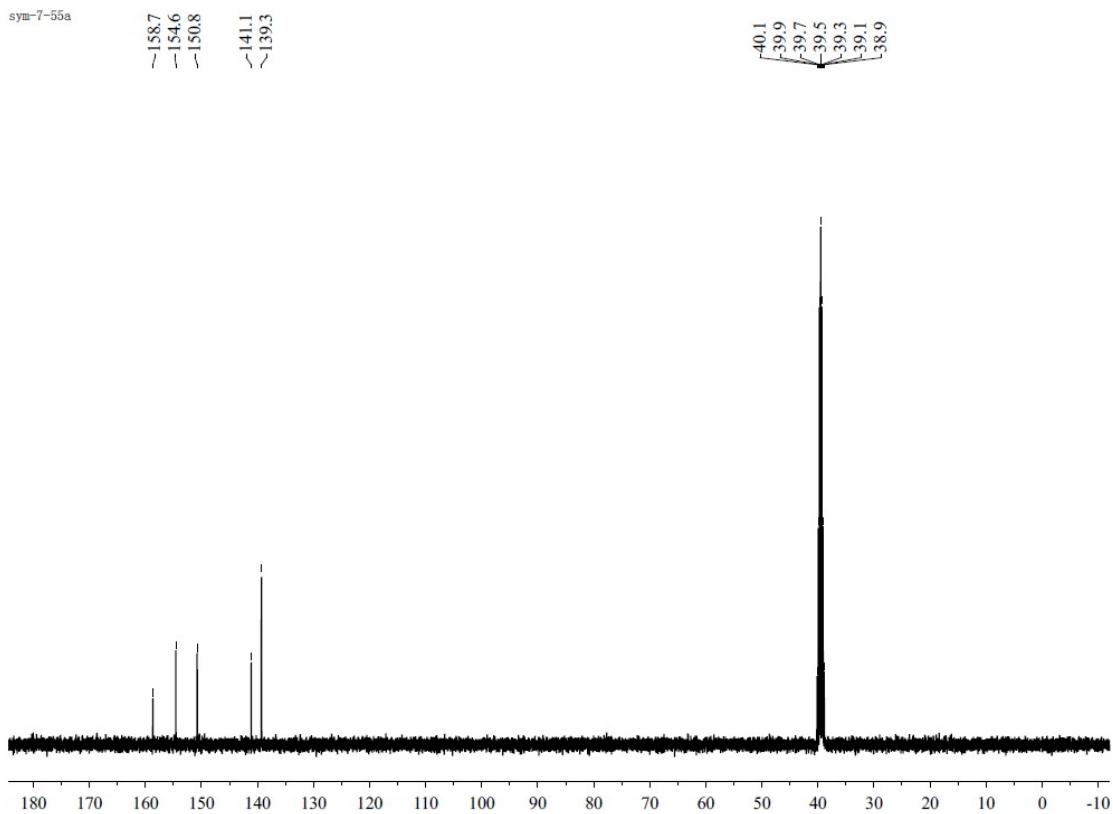


Figure S13.  $^1\text{H}$  NMR spectrum of bis(3-amino-1,2,4-triazolium) BNOA (**12**)

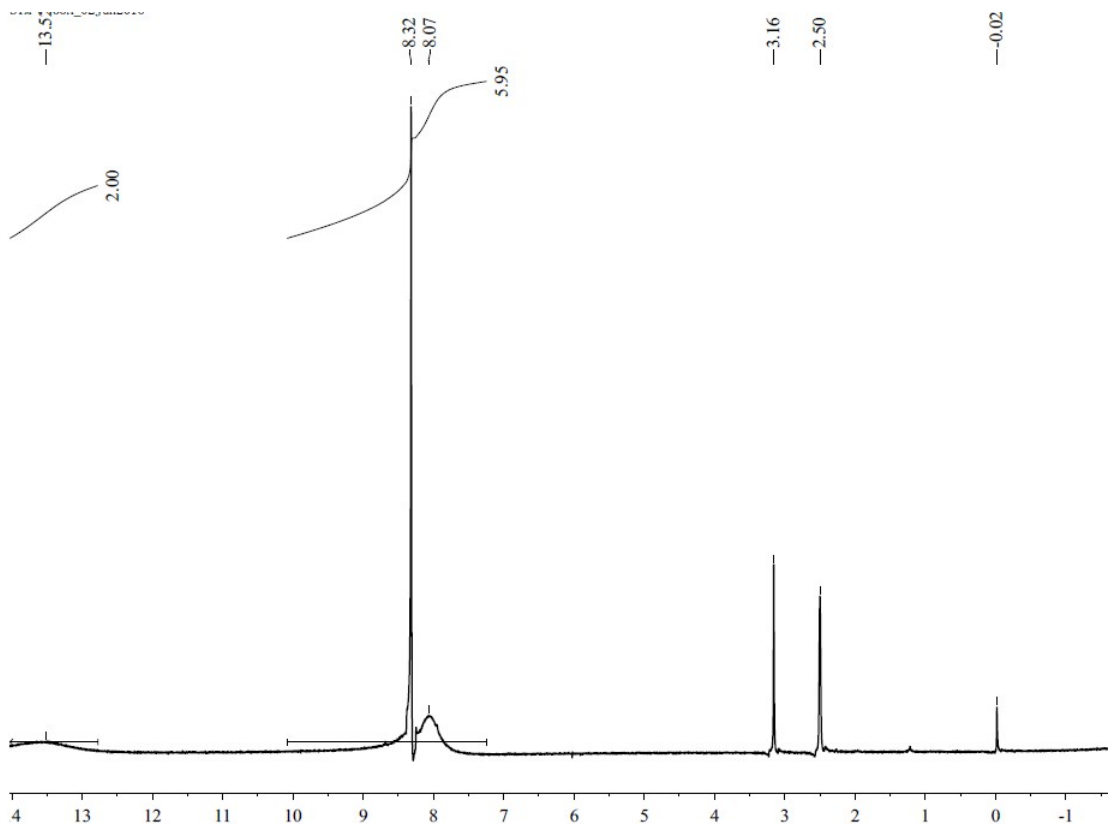


Figure S14.  $^{13}\text{C}$  NMR spectrum of bis(3-amino-1,2,4-triazolium) BNOA (**12**)

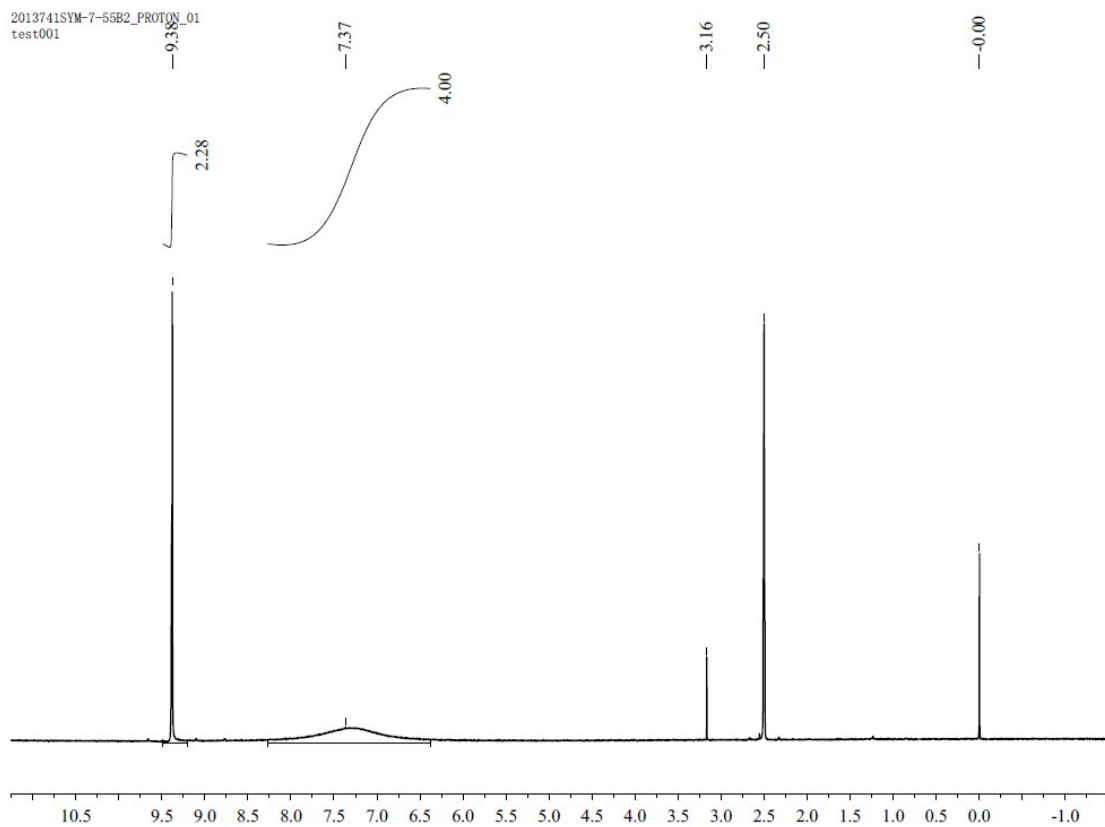


Figure S15.  $^1\text{H}$  NMR spectrum of bis(4-amino-1,2,4-triazolium) BNOA (**13**)

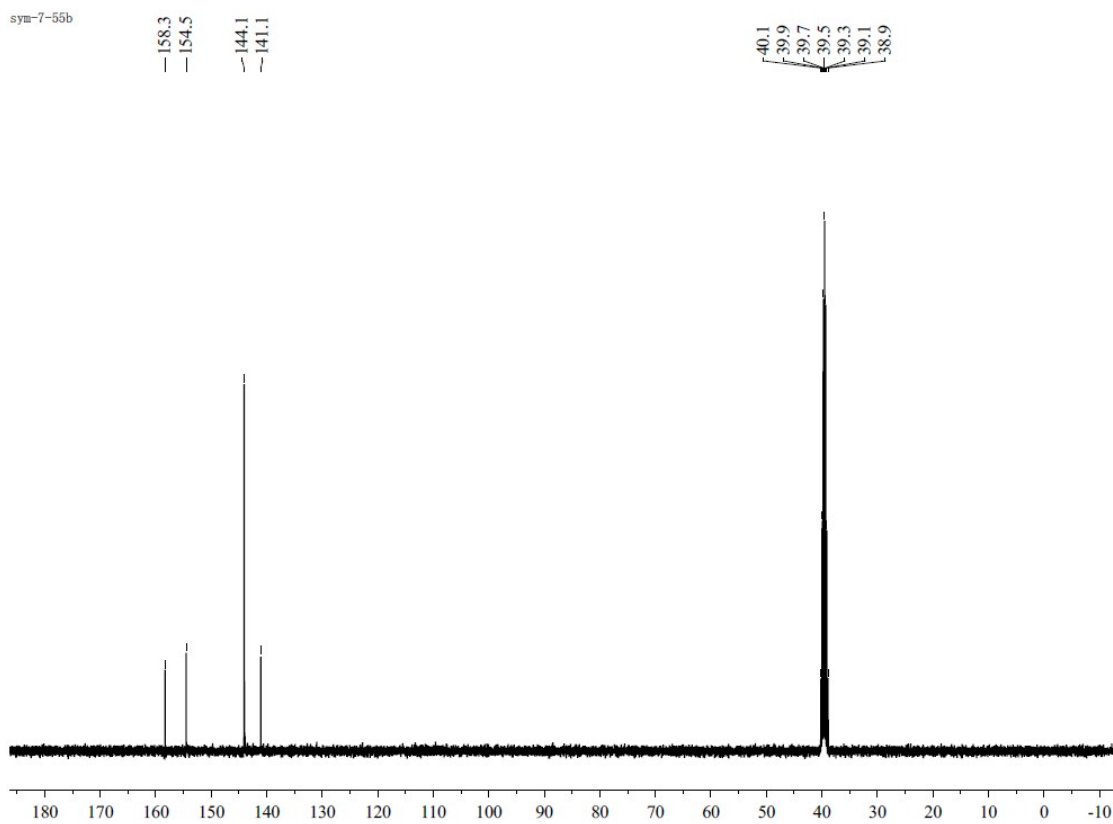


Figure S16.  $^{13}\text{C}$  NMR spectrum of bis(4-amino-1,2,4-triazolium) BNOA (**13**)

## 2. Crystallographic data

Table S1 Crystallographic data and structure refinement parameters for **5**, **7**, **8** and **13**<sup>[a]</sup>.

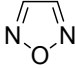
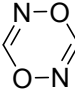


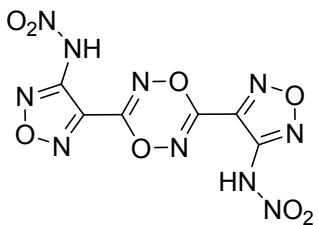
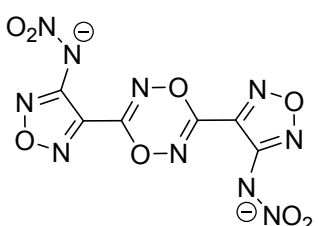
	<b>5</b>	<b>6</b>	<b>8</b>	<b>13</b>
CCDC number	1495666	1495667	1495668	1495669
Empirical formula	C <sub>6</sub> H <sub>2</sub> N <sub>10</sub> O <sub>8</sub>	C <sub>6</sub> H <sub>10</sub> N <sub>12</sub> O <sub>9</sub>	C <sub>6</sub> H <sub>8</sub> N <sub>12</sub> O <sub>10</sub>	C <sub>10</sub> H <sub>10</sub> N <sub>8</sub> O <sub>3</sub>
<i>M</i> <sub>w</sub>	342.18	394.26	408.24	510.36
Crystal system	Trigonal	Triclinic	Monoclinic	Monoclinic
Space group	R-3:H	P-1	P1 21/c 1	P 21/c
<i>a</i> [Å]	24.929(3)	8.327(3)	12.4121(19)	8.248(2)
<i>b</i> [Å]	24.929(3)	8.515(3)	4.1853(7)	16.509(4)
<i>c</i> [Å]	5.2298(9)	10.354(3)	14.866(2)	7.2536(17)
$\alpha$ [°]	90	85.243(7)	90	90
$\beta$ [°]	90	83.980(7)	113.460(3)	97.398(5)
$\gamma$ [°]	120	85.302(7)	90	90
<i>V</i> [Å <sup>3</sup> ]	2814.7(9)	725.6(4)	708.5(2)	979.5(4)
<i>Z</i>	9	2	2	2
<i>T</i> [K]	293(2)	293(2)	130	293(2)
$\lambda$ [Å]	0.71073	0.71073	0.71073	0.71073
Density[ $\text{mg m}^{-3}$ ]	1.817	1.805	1.914	1.730
$\mu$ [ $\text{mm}^{-1}$ ]	0.168	0.166	0.179	0.150
<i>F</i> (000)	1548	404	416	520
Crystal size[ $\text{mm}^{-3}$ ]	0.180×0.110×0.0	0.20×0.14×0.	0.15×0.12×0.	0.200×0.160×0.1
$\theta$ range[°]	80	10	05	20
Index ranges	2.830-24.958	1.983-24.997	1.789-30.617	2.467-25.499
	-29≤ <i>h</i> ≤29	-9≤ <i>h</i> ≤9	-17≤ <i>h</i> ≤13	-9≤ <i>h</i> ≤9
	-29≤ <i>k</i> ≤22	-10≤ <i>k</i> ≤10	-5≤ <i>k</i> ≤5	-20≤ <i>k</i> ≤14
	-6≤ <i>l</i> ≤6	-12≤ <i>l</i> ≤9	-17≤ <i>l</i> ≤21	-8≤ <i>l</i> ≤8
Reflections collected	5145	4026	6729	5442
Independent reflections	1091	2552	2164	1821
	[ <i>R</i> (int)=0.0416]	[ <i>R</i> (int)=0.0281]	[ <i>R</i> (int)=0.0309]	[ <i>R</i> (int)=0.0320]
Data/restraints/parameters	1091/0/114	2552/22/284	2164/0/143	1821/0/175
GOF	1.108	1.041	1.022	1.080
<i>R</i> [ <i>F</i> <sup>2</sup> > 2σ( <i>F</i> <sup>2</sup> )]	0.0403	0.0760	0.0396	0.0448
<i>wR</i> ( <i>F</i> <sup>2</sup> ) <sup>[b]</sup>	0.0971	0.2047	0.0933	0.1085

[a] These data can be obtained free of charge from The Cambridge Crystallographic Data Centre via [www.ccdc.cam.ac.uk/data\\_request/cif](http://www.ccdc.cam.ac.uk/data_request/cif).

### 3 Ab Initio computational data

Table S2 Ab Initio computational data.

Compounds	<i>E</i> <sub>0</sub> (Hartree)	ZPE (Hartree)	<i>H</i> <sub>T</sub> (Hartree)	HOF (kJ/mol)
	-261.532452	0.045697	0.004418	196.75 <sup>[1]</sup>
CH <sub>4</sub>	-40.3984857	0.044793	0.003812	-74.6 <sup>[2]</sup>
NH <sub>3</sub>	-56.4341763	0.034372	0.003818	-45.9 <sup>[2]</sup>
CH <sub>3</sub> NH <sub>2</sub>	-95.6318759	0.064032	0.004369	-23.0 <sup>[2]</sup>
NH <sub>2</sub> NO <sub>2</sub>	-260.5478787	0.039257	0.003356	-6.1 <sup>[3]</sup>
	-336.5623427	0.048881	0.004895	163.5
CH <sub>3</sub> CH <sub>3</sub>	-79.6068548	0.00443	0.070179	-84.68 <sup>[4]</sup>

	-1376.0491004	0.139621	0.020139	592.2
	-1374.9582833	0.112786	0.01964	324.3

<sup>a</sup> Total energy ( $E_0$ ) calculated by B3LYP/6-31+G\*\*/MP2/6-311++G\*\* method (Hartree/Particle);

<sup>b</sup> Zero-point correction (ZPE) (Hartree/Particle); <sup>c</sup> Values of thermal correction ( $H_T$ )

(Hartree/Particle); <sup>d</sup> Heat of formation (HOT) (kJ/mol).

Calculations were carried out by using the Gaussian 09 (Revision E.01) suite of programs.<sup>[4]</sup> The geometric optimization of the structures and frequency analyses were carried out by using the B3LYP functional with the 6-31+G\*\* basis set, and single-point energies were calculated at the MP2(full)/6-311++G\*\* level. All of the optimized structures were characterized to be true local energy minima on the potential-energy surface without imaginary frequencies.

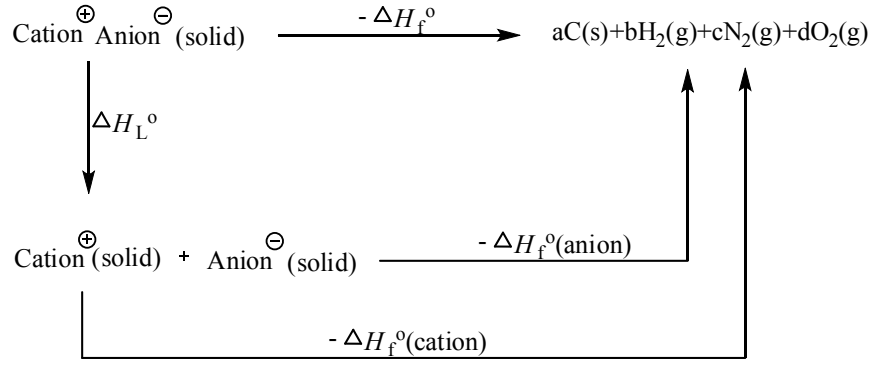


Figure S15. Born-Haber cycle for the formation for energetic salts

Based on the Born-Haber energy cycle (Figure 5), the heat of formation of a salt can be simplified according to Equation (1), where  $\Delta H_L$  is the lattice energy of the salt.

$$\Delta H_f^{\circ}(\text{ionic salt, 298K}) = \Delta H_f^{\circ}(\text{cation, 298K}) + \Delta H_f^{\circ}(\text{anion, 298K}) - \Delta H_L \quad (1)$$

The  $\Delta H_L$  value could be predicted by the formula suggested by Jenkins et al [Eq. (2)],<sup>[5]</sup> where  $U_{\text{POT}}$  is the lattice potential energy and  $nM$  and  $nX$  depend on the nature of the ions  $M^{p+}$  and  $X^{q-}$ , respectively, and are equal to three for monoatomic ions, five for linear polyatomic ions, and six for nonlinear polyatomic ions.

$$\Delta H_L = U_{\text{POT}} + [p(n_M/2-2) + q(n_X/2-2)]RT \quad (2)$$

The equation for the lattice potential energy,  $U_{\text{POT}}$ , takes the form of Equation (3), where  $\rho_m$  is the density ( $\text{g cm}^{-3}$ ),  $M_m$  is the chemical formula mass of the ionic material ( $\text{g}$ ), and the coefficients  $\gamma$  ( $\text{kJ}^{-1}\text{mol}^{-1}\text{cm}$ ) and  $\delta$  ( $\text{kJ}^{-1}\text{mol}^{-1}$ ) are assigned literature values.<sup>[5]</sup>

$$U_{\text{POT}}(\text{kJ}^{-1}\text{mol}^{-1}) = \gamma (\rho_m/M_m)^{1/3} + \delta \quad (3)$$

#### 4 Detonation performances calculation

Detonation pressure ( $P$ ) and detonation velocity ( $D$ ) were calculation according to the Kamlet-Jacobs

equations<sup>[5]</sup>.

$$D = 1.01(N \bar{M}^{1/2} Q^{1/2})^{1/2}(1 + 1.30\rho) \quad (4)$$

$$P = 1.558\rho^2 \bar{M}^{1/2} Q^{1/2} \quad (5)$$

where each term in eqs 4 and 5 is defined as follows:  $D$ , the detonation velocity ( $\text{km s}^{-1}$ );  $P$ , the detonation pressure (GPa);  $N$ , the moles of detonation gases per gram explosive;  $\bar{M}$ , the average molecular weight of these gases ( $\text{g mol}^{-1}$ );  $Q$ , the heat of detonation ( $\text{J g}^{-1}$ ); and  $\rho$ , the loaded density of explosives ( $\text{g cm}^{-3}$ ). The measured density was used for the calculation here.

- 
- 1 Wang R, Guo Y, Zeng Z, et al. *Chem. Eur. J.*, 2009, 15, 2625-2634.
  - 2 *Eur. J. Inorg. Chem.*, 2008, 2560-2568.
  - 3 Wang K, Parrish D A, Shreeve J M. *Chem. Eur. J.*, 2011, 17, 14485-14492.
  - 4 *New J. Chem.*, 2008, 32, 317-322.
  - 5 (a) M. J. Kamlet, S. J. Jacobs, *J. Chem. Phys.* **1968**, 48, 23-35; (b) M. J. Kamlet, J. E. Ablard, *J. Chem. Phys.* **1968**, 48, 36-42; (c) M. J. Kamlet, C. Dicknison, *J. Chem. Phys.* **1968**, 48, 43-49. (d) H. Gao, C. Ye, C. Piekarski, J. M. Shreeve, *J. Phys. Chem. C* **2007**, 111, 10718-10731.